

Accumulation of nonlinear interference noise in fiber-optic systems

Ronen Dar, Meir Feder, Antonio Mecozzi, and Mark Shtaif

Abstract—We show that the analytical results provided in Ref. [6] accurately predict the accumulation of nonlinear interference noise (NLIN) in fiber-optic communications systems. Our results demonstrate that all of the previously not understood discrepancies between the Gaussian noise (GN) model and simulations can be attributed to the omission of an important fourth-order noise (FON) term that correctly accounts for the statistical dependencies within the spectrum of the interfering channel. We provide a computationally efficient method for evaluating the FON contribution, as well as the overall NLIN power.

I. INTRODUCTION

Inter-channel nonlinear interference is arguably the most important factor in limiting the performance of fiber-optic communications [1]. Since joint processing of the entire WDM spectrum of channels is prohibitively complex, nonlinear interference between channels is customarily treated as noise. The statistical characterization of this noise — to which we refer in what follows as nonlinear interference noise (NLIN) — is the goal of most recent theoretical studies of nonlinear transmission [2]–[8]. Understanding the features of NLIN is critical for the efficient design of fiber-optic systems and for the accurate prediction of their performance.

Most of the available work on NLIN in fiber-optic systems was published in the context of the Gaussian noise (GN) model [2]–[5], which describes NLIN as an additive Gaussian noise process whose variance and spectrum it evaluates. The validation of the GN model and the characterization of its accuracy have been the subject of numerous studies (e.g. see [3], [4]). It was found that while the model’s accuracy is satisfactory in some scenarios, it is highly inadequate in others. Some of the GN model’s most conspicuous shortcomings are its independence of modulation format [6], its independence of pre-dispersion [4], and its large inaccuracy in predicting the growth of the NLIN variance with the number of spans in an amplified multi-span link [3], [4]. Although phenomenological fixes for the latter problem have been proposed (either by means of parameter fitting or by accumulating the NLIN contributions of various spans incoherently), the remedy that they offered remained limited, and the fundamental reason for the observed behavior has never been understood.

In this paper we show that the theory introduced in Sect. 3 of [6] resolves all of the above mentioned discrepancies and accurately predicts the accumulation of NLIN in generic transmission scenarios. Following up on [6], we argue that the reason for the inaccuracy of the GN approach is in ignoring the statistical dependence between different frequency

R. Dar, M. Feder, and M. Shtaif are with the School of Electrical Engineering, Tel Aviv University, Tel Aviv 69978, Israel. A. Mecozzi is with the Department of Physical and Chemical Sciences, University of L’Aquila, L’Aquila 67100, Italy.

components of the interfering channel. Accounting for this dependence produces an important correction term to which we refer (for reasons explained in the following section) as the *fourth-order noise* or FON. We demonstrate in what follows that the FON term resolves all the current inaccuracies of the GN model, including the dependence on modulation format, signal pre-dispersion, and the accumulation of NLIN with the number of spans.

We stress that as demonstrated in [6] the NLIN is not an additive Gaussian process, and hence its variance (and even its entire spectrum) does not characterize its properties in a satisfactory manner. For example, as pointed out in [7], part of the NLIN manifests itself as phase-noise, whose effect in terms of transmission performance is very different from that of additive noise [9]. We show in what follows that the phase-noise character of NLIN, as well as the dependence of NLIN on modulation format is largest in the case of a single amplified span, or in a system of arbitrary length that uses distributed amplification (as in [6]). The distinctness of these properties reduces somewhat in multi-span systems with lumped amplification and with a span-length much larger than the fiber’s effective length.

Finally, in order to facilitate future research of this problem, we provide a matlab code that implements a computationally efficient algorithm for computing the FON, as well as the complete variance of the NLIN.

II. THEORETICAL BACKGROUND

In a recent paper [6] we have demonstrated that by removing the assumption of statistical independence between frequency components within the interfering channel (which has been used in the derivation of the GN model) the variance of NLIN is given by

$$\sigma_{\text{NLIN}}^2 = \underbrace{P^3 \chi_1}_{\text{SON}\backslash\text{GN}} + \underbrace{P^3 \chi_2 \left(\frac{\langle |b|^4 \rangle}{\langle |b|^2 \rangle^2} - 2 \right)}_{\text{FON}}, \quad (1)$$

where P is the average power, b denotes the data symbol in the interfering channel (e.g. for QPSK modulation b is a random variable that receives each of the four values $\pm \frac{1}{\sqrt{2}} \pm \frac{i}{\sqrt{2}}$ with probability of 1/4), and the angled brackets denote statistical averaging. The terms χ_1 and χ_2 are given by Eqs. (26–27) in [6] multiplied by T^3 , where T is the symbol duration. These coefficients are functions of the transmitted pulse waveform and of the fiber parameters. The first term on the right-hand-side of (1) is identical to the result of the GN model, and since it follows only from second-order statistics, we refer to it as the second-order noise (SON) term. The second term depends

on fourth-order statistics and is hence referred to as the fourth-order noise (FON) term. The presence of $\langle |b|^4 \rangle$ in the FON term implies modulation format dependence. For example, the NLIN variance is $P^3(\chi_1 - \chi_2)$ with QPSK modulation, $P^3(\chi_1 - 0.68\chi_2)$ with 16-QAM, and $P^3\chi_1$ when Gaussian modulation is used. Note that only with Gaussian modulation the NLIN variance is independent of χ_2 and hence the GN-model's prediction is exact. In the section that follows we demonstrate the accuracy of Eq. (1) with respect to a range of fiber-optic systems that we simulate, and discuss the role and relative importance of the FON term in the various scenarios.

III. RESULTS AND DISCUSSION

The results are obtained from a series of simulations considering a five-channel WDM system implemented over standard single-mode fiber (dispersion of 17 ps/nm/km, nonlinear coefficient $\gamma = 1.3$ [Wkm] $^{-1}$, and attenuation of 0.2dB per km). We assume Nyquist pulses with a perfectly square spectrum, a symbol-rate of 100 Gb/s and a channel spacing of 102 GHz, as in [1]. The number of simulated symbols in each run was 16384 and up to 500 runs (each with independent and random data symbols) were performed with each set of system parameters, so as to accumulate sufficient statistics. As we are only interested in characterizing the NLIN, we did not include amplified spontaneous emission (ASE) noise in any of the simulations. At the receiver, the channel of interest was isolated with a matched optical filter and back-propagated so as to eliminate the effects of self-phase-modulation and chromatic dispersion.

In Fig. 1 we show the NLIN power as a function of the average input power for a system consisting of 5×100 km spans in the cases of QPSK and 16-QAM modulation. Figure 1a corresponds to the case of purely distributed amplification, which has been addressed in [6], and is shown here only for reference. Figure 1b represents the same system in the case of lumped amplification. The solid curves represent the analytical results obtained from Eq. (1), whereas the dots represent the results of the simulations. The dashed red curve shows the prediction of the GN model, i.e. $P^3\chi_1$. The dependence on modulation format is evident in both figures, as is the GN model's offset. However, while the error of the GN model in the case of QPSK is 6.5dB in the case of distributed amplification, it reduces to 2.7dB when lumped amplification is used. Note that the difference between the modulation formats, as well as the error of the GN-model result are both independent of the input power. The excellent agreement between the theory (Eq. (1)) and simulation is self evident.

More insight as to the significance of the span-length can be extracted from Fig. 2 which shows the received constellations in a 500 km system for QPSK (left panels) and 16-QAM (right panels) transmission. The top panels (Figs. 2a and 2b) correspond to the case of 25 km spans, the middle panels (Figs. 3c and 3d) correspond to 50 km spans and the case of 100 km spans is shown in the bottom panels (Figs. 2e and 2f). Here and in the figures that follow, the injected powers were selected such that the path-averaged power was -6dBm in all cases (input power of -3.7dBm, -1.9dBm and 0.7dBm, for 25 km, 50 km, and 100 km spans, respectively). Use of a

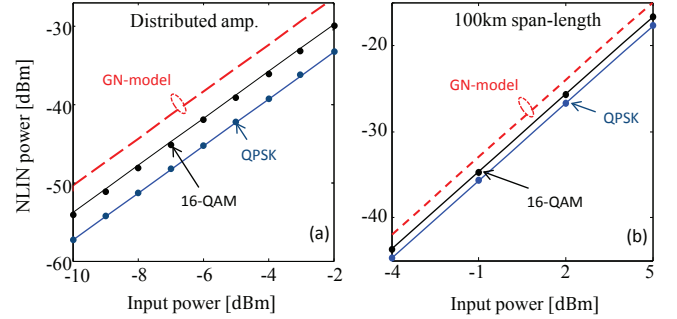


Fig. 1. The NLIN power versus the average power per-channel in a 5×100 km system for QPSK and 16-QAM modulation. The solid lines show the theoretical results given by Eq. (1) and the dots represent simulations. The dashed red line corresponds to the SON contribution $P^3\chi_1$, which is identical to the result of the GN model. (a) Distributed amplification [6]. (b) Lumped amplification.

constant path-averaged power is customary when comparing systems with different span lengths [10], and the value of -6 dBm was found to be roughly optimal from the standpoint of capacity maximization in the distributed amplification case [9], [11]. As can be seen in Fig. 1, the comparison between modulation formats is practically independent of the launched optical power. Consistently with the predictions in [6], the phase noise is negligible in the case of QPSK transmission, and the constellation points are nearly circular for all span-lengths. With 16-QAM modulation phase-noise is dominant in the case of 25 km spans, whereas at longer span-lengths the phase-noise character of NLIN becomes less evident. We note that even in the case of 100 km spans, phase noise is clearly visible implying that NLIN cannot be accurately described as additive, although the error from doing so is notably smaller.

Figure 3 shows the accumulation of NLIN along systems of different span-lengths. In Figs. 3a-3c, the span-lengths are 25 km, 50 km, and 100 km, respectively. The NLIN power in these figures is normalized to the received optical power in each case so that the vertical axes can be interpreted as noise to signal ratio. Notice that in the cases of single-span transmission the dependence on modulation format and the inaccuracy of the GN model are largest. As the number of spans increases the NLIN increases more rapidly for the QPSK format and the difference between the modulation formats reduces. After 500 km of propagation the difference between the NLIN power for QPSK and 16-QAM modulation formats is approximately 3dB, 2.5dB, 1.6dB and 1dB for distributed amplification, 25 km, 50 km, and 100 km spans (the result for the case of distributed amplification is extracted from Fig. 1a). The error of the GN model in the case of QPSK is approximately 6.5dB, 5.8dB, 4.1dB, and 2.7dB for the cases of distributed amplification, 25 km, 50 km and 100 km spans. The effect of signal pre-dispersion is also accurately accounted for by our theory, as demonstrated in Fig. 3d. Here the injected pulses are pre-dispersed by 850 ps/nm and — consistently with what has been recently observed in [4] — the simulated NLIN variance is seen to approach the GN-model's result when the number of spans is small, but then unlike in [4] (where the amount of pre-dispersion was significantly larger) it deviates

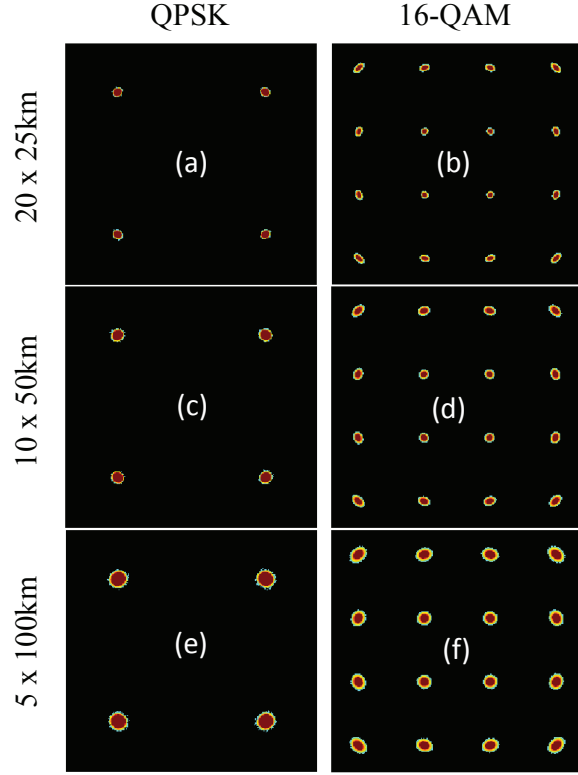


Fig. 2. Constellation diagrams for QPSK (left panels) and 16-QAM (right panels) in the cases of 25 km spans (a and b), 50 km (c and d) and 100 km (e and f). In all cases a path-averaged power of -6dBm was used. The phase noise nature of NLIN is evident in the case of 16-QAM modulation, but its relative significance reduces when the span-length is large. The 100 km span case is closer to the circular noise distributions observed in [3].

from it when the span-number grows towards 10.

The explanation to the observed behavior can be attributed to the dynamics of nonlinear collisions in WDM systems, whose details will be discussed in a separate publication. In particular, NLIN that is induced by cross-phase-modulation (XPM) is strongest when the nonlinearly interacting pulses experience incomplete collisions [12]. In a single-span system, or in a system with distributed gain, such collisions occur only twice; once in the beginning of the system and again at its end. In a multi-span system with lumped amplification incomplete collisions occur at every point of power discontinuity, namely at the beginning of every amplified span. The significance of the incomplete collisions grows both with their number and with the magnitude of the power discontinuity. For a fixed link-length the accumulated effect of incomplete collisions grows with the shortening of the span length (i.e., with the number of spans), up to the point where the span length becomes comparable with the fiber's effective length (~ 20 km in standard fibers). Beyond this point the magnitude of the power discontinuity reduces and the system gradually approaches the regime of distributed amplification. Incomplete collisions taking place at different locations produce NLIN contributions of independent phase and therefore, when the NLIN is dominated by incomplete collisions, it appears more isotropic in phase-space and its distribution becomes closer to Gaussian. This is the reason for the fact that the NLIN

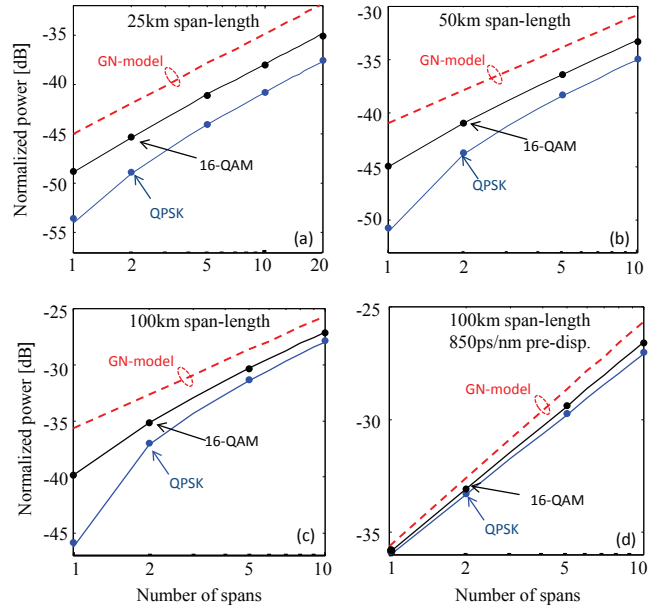


Fig. 3. Accumulation of the NLIN power (normalized to the received power) with the number of spans. Figures a,b and c correspond to span-lengths of 25 km, 50 km, and 100 km, respectively. In Fig. 3d, which also corresponds to 100 km spans, pre-dispersion of 850 ps/nm was applied to the injected pulses. The solid lines show the theoretical results given by Eq. (1) and the dots represent simulations. The red dashed curve represents the SON, or equivalently the GN model result.

in Fig. 2f is stronger and more circular than in Fig. 2b, or 2d, in which the contribution of incomplete collisions is much smaller. This is also the reason for the fact that the dependence on modulation format in Figs. 3a-3c reduces with the number of spans, and the NLIN variance gradually approach to the GN-result.

The collisions picture also explains the fact that in the presence of aggressive pre-dispersion ([4] and Fig. 3d) the NLIN variance is closer to the GN model's predictions. This is simply a consequence of the fact that the temporal spreading of the launched pulses becomes larger than the walk-off between channels, so that all collisions are incomplete. Interestingly, when the number of spans grows (e.g. consider the case of 5 to 10 spans in Fig. 3d), so that the channel walk-off becomes comparable to the initial pulse-spread and complete collisions reappear, the deviation from the GN-result emerges once again. This suggests that it is not the improved Gaussianity that causes the NLIN variance to be closer to the GN prediction (as claimed in [4]), but the collision dynamics discussed above. Namely, when the link is short enough for the inter-channel walk-off to become much smaller than the initial pulse-spreading, complete collisions do not occur and the GN result gains accuracy. When examining the situation in the frequency domain, pre-dispersion implies rapid phase variations in the interfering channel's spectrum (i.e. variations in the phase of $\tilde{g}(\omega)$ in the notation of [6]). While the SON coefficient χ_1 is not affected by the spectral phase, the FON coefficient χ_2 reduces considerably in this situation, since the fourth-order correlation terms (Eq. 24 in [6]) lose coherence. We note however, that since with all relevant modulation formats, the

quantity $\frac{\langle |b|^4 \rangle}{\langle |b|^2 \rangle^2} - 2$ is negative, the reduction of χ_2 through pre-dispersion always leads to an increase in the NLIN variance and is therefore undesirable.

IV. CONCLUSIONS

We have shown that the previously unexplained dependence of the NLIN variance on pre-dispersion, modulation format and on the number of amplified spans is accounted for by the FON term, which follows from the correct treatment of the signal's statistics [6]. The relative magnitude of the FON term is largest in single span systems, or in systems using distributed amplification, and it reduces notably in the case of lumped amplification with a large number of spans.

V. ACKNOWLEDGEMENT

The authors would like to acknowledge financial support from the Israel Science Foundation (grant 737/12). Ronen Dar would like to acknowledge the support of the Adams Fellowship of the Israel Academy of Sciences and Humanities, and the Yitzhak and Chaya Weinstein Research Institute.

APPENDIX: COMPUTATION OF χ_1 AND χ_2

The extraction of the analytical curves in Figs. 1 and 2 relies on the computation of the SON and FON coefficients χ_1 and χ_2 , which requires summation over three and five indices, respectively. Multi-dimensional summations are very inefficient in brute-force computation, and hence we use the Monte-Carlo integration method [13] for evaluating these quantities. We provide a matlab code that computes χ_1 , χ_2 , the implied NLIN variance according to Eq. (1), and the relative error in the computed variance. In all our numerical evaluations the number of runs N was large enough to ensure that the relative error was smaller than 3%. The program assumes perfect Nyquist pulses, but it can be readily extended to an arbitrary pulse-shape.

```
% System parameters
gamma = 1.3; % nonlinear coeff. in W^-1*km^-1
beta2 = 21; % dispersion coeff. in ps^2/km
alpha = 0.2/10*log(10); % fiber loss coeff. in 1/km
Nspan = 10; % number of spans
L = 100; % span length in km
PD = 500*beta2; % pre-dispersion length in ps^2
PdBm = 0.7; % input average power in dBm
BW = 100; % bandwidth of the signal in GHz
T=1000/BW; % symbol duration in ps
carr = 102; % channel spacing in GHz
kur = 1.32; % modulation factor <|b|^4>/<|b|^2>^2
N = 5000000; % number of points

% Monte-Carlo integration
P0 = 10^((PdBm-30)/10);
q = carr./BW;
beta2 = beta2/T^2;
R = 2*pi*(rand(4, N)-0.5*ones(4, N));
Volume = (2*pi)^4;
% calculate X1
arg1 = (R(2,:)-R(3,:)).*(R(1,:)-2*pi*q-R(3,:));
argPD1 = arg1;
ss1 = exp(li*argPD1*PD).*exp(li*beta2*arg1...
    *L-alpha*L)-1./((li*beta2*arg1-alpha));
s1 = abs(ss1.*((1-exp(li*Nspan*arg1*beta2*L))...
    ./(1-exp(li*arg1*beta2*L))).^2/(2*pi)^4);
avgF1 = sum(s1)/N;
X1 = avgF1*Volume*(4*gamma^2*P0^3);
% calculate X2
```

```
arg21 = (R(2,:)-R(3,:)).*(R(1,:)-2*pi*q-R(4,:));
arg22 = (R(2,:)-R(3,:)+2*pi).*((R(1,:)-2*pi*q-R(4,:));
arg23 = (R(2,:)-R(3,:)-2*pi).*((R(1,:)-2*pi*q-R(4,:));
arg2 = [arg21; arg22; arg23];
arg31 = (R(4,:)-R(3,:)+R(2,:)<pi)...*...
    .*(R(4,:)-R(3,:)+R(2,:)>-pi);
arg32 = (R(2,:)-R(3,:)+R(4,:)+2*pi<pi)...*...
    .*(R(2,:)-R(3,:)+R(4,:)+2*pi>-pi);
arg33 = (R(2,:)-R(3,:)+R(4,:)-2*pi<pi)...*...
    .*(R(2,:)-R(3,:)+R(4,:)-2*pi>-pi);
arg3 = [arg31; arg32; arg33];
argPD21 = (R(2,:)-R(3,:)).*(R(1,:)-2*pi*q-R(4,:));
argPD22 = (R(2,:)-R(3,:)+2*pi).*((R(1,:)-2*pi*q-R(4,:));
argPD23 = (R(2,:)-R(3,:)-2*pi).*((R(1,:)-2*pi*q-R(4,:));
argPD2 = [argPD21; argPD22; argPD23];
s2=0;
for ind=1:3
    ss2 = exp(-li*argPD2(ind,:)*PD).*...
        (exp(-li*beta2*arg2(ind,:)*L-alpha*L)-1)...*...
        ./(-li*beta2*arg2(ind,:)-alpha);
    s2 = s2 + (1-exp(li*Nspan*arg1*beta2*L))...
        ./((1-exp(li*arg1*beta2*L)).*ss1*...
        .*((1-exp(-li*Nspan*arg2(ind,:)*beta2*L))...*...
        ./((1-exp(-li*arg2(ind,:)*beta2*L)).*ss2*...
        /(2*pi)^4.*arg3(ind,:));
end
avgF2 = real(sum(s2))/N;
X2 = avgF2*Volume*(4*gamma^2*P0^3);
NLIN_var = X1+((kur-2)*X2); % in W
% calculate the root mean square relative error
Err = ((sum((s1-avgF1+((kur-2)*(real(s2)-avgF2))...*...
    .^2)/(N-1))^2/(avgF1+((kur-2)*avgF2))/sqrt(N));
```

REFERENCES

- [1] R.-J. Essiambre, G. Kramer, P.J. Winzer, G.J. Foschini, B. Goebel, "Capacity limits of optical fiber networks," *J. Lightwave Technol.*, vol. 28, pp. 662–701, (2010).
- [2] P. Poggiolini, A. Carena, V. Curri, G. Bosco, F. Forghieri, "Analytical modeling of nonlinear propagation in uncompensated optical transmission links," *IEEE Photon. Technol. Lett.*, vol. 23, pp. 742–744, (2011).
- [3] A. Carena, V. Curri, G. Bosco, P. Poggiolini, F. Forghieri, "Modeling of the impact of nonlinear propagation effects in uncompensated optical coherent transmission links," *J. Lightwave Technol.*, vol. 30, pp. 1524–1539 (2012).
- [4] A. Carena, G. Bosco, V. Curri, P. Poggiolini, F. Forghieri, "Impact of the transmitted signal initial dispersion transient on the accuracy of the GN-model of non-linear propagation," 39th European Conference and Exhibition on Optical Communication (ECOC 2013), Paper Th.1.D.4.
- [5] P. Johannsson and M. Karlsson, "Perturbation analysis of nonlinear propagation in a strongly dispersive optical communication system," *IEEE J. Lightwave Technol.*, vol. 31, pp. 1273–1282 (2013).
- [6] R. Dar, M. Feder, A. Mecozzi, M. Shtaif, "Properties of nonlinear noise in long, dispersion-uncompensated fiber links," *Optics Express*, vol. 21, pp. 25685–25699, (2013).
- [7] A. Mecozzi and R.-J. Essiambre, "Nonlinear Shannon limit in pseudo-linear coherent systems," *J. Lightwave Technol.*, vol. 30, pp. 2011–2024 (2012).
- [8] M. Secondini, E. Forestieri, G. Prati, "Achievable information rate in nonlinear WDM fiber-optic systems with arbitrary modulation formats and dispersion maps," *J. Lightwave Technol.*, vol. 31, pp. 3839–3852, (2013).
- [9] R. Dar, M. Shtaif, M. Feder, "New bounds on the capacity of the nonlinear fiber-optic channel," *Optics Lett.*, vol. 39, pp. 398–401 (2014).
- [10] J. P. Gordon and L. F. Mollenauer, "Effects of fiber nonlinearities and amplifier spacing on ultra-long distance transmission," *J. Lightwave Technol.*, vol. 9, pp. 170–173, (1991).
- [11] R. Dar, M. Shtaif, M. Feder, "Improved bounds on the nonlinear fiber-channel capacity," 39th European Conference and Exhibition on Optical Communication (ECOC 2013), Paper P.4.16.
- [12] M. Shtaif, "Analytical description of cross-phase modulation in dispersive optical fibers," *Optics Lett.*, vol. 23, pp. 1191–1193, (1998).
- [13] R. E. Caflisch, "Monte Carlo and quasi-Monte Carlo methods," *Acta Numerica* vol. 7, Cambridge University Press, pp. 1–49 (1998).